

Modeling a membrane reactor for a zero-emission combined cycle power plant

Janusz Kotowicz*, Marcin Job*

Institute of Power Engineering and Power Turbomachinery, Silesian University of Technology, Konarskiego 18, 44-100 Gliwice, Poland;

Abstract

A zero emission gas turbine power plant with a membrane reactor works on the concept of using ion oxygen transport membrane (ITM) technology in order to apply carbon dioxide capture with limited loss of electricity generation efficiency. The membrane reactor replaces the combustor in the gas turbine and combines three functions: oxygen separation from air through a high-temperature membrane, fuel combustion in the internal reactor cycle, and heating oxygen-depleted air, which is directed to the turbine. This paper presents a gas turbine power plant integrated with a membrane reactor and a detailed description of the membrane reactor model. Selected results of thermodynamic analysis of the modeled power plant are presented.

Keywords: oxy-combustion; zero-emission combined cycle gas turbine; membrane reactor; ion transport membrane; ITM

1. Introduction

The world energy sector is facing the challenge of reducing greenhouse gas emissions, in particular carbon dioxide, out of concerns over climate change [1]. The main source of emissions is the combustion of fossil fuels, therefore, carbon capture and storage (CCS) technologies are being developed. The application of these technologies is intended to allow fossil fuel power plants to operate at zero or nearly zero CO₂ emissions. The most favorable fossil fuel from the ecological point of view is natural gas, which has seen an increase in global consumption in recent years, hand-in-hand with the rapid development of combined cycle power plants (CCPP). Despite their numerous advantages, CCS technologies are expected to be applied in CCPP in order to maintain their competitiveness with respect to other electricity generation technologies [2–4].

Three groups of CCS technologies can be distinguished: pre-combustion, post-combustion and oxy-combustion. The oxy-combustion technology is based on elimination of nitrogen from the combustion process. Carbon dioxide capture from flue gases, consisting mainly of CO₂ and H₂O, requires only flue gas cooling and condensation of excess water. However, the biggest challenge for oxy-combustion power plants is the need to produce a high amount of oxygen. The only recently available technique providing oxygen with

the required quantity and quality is cryogenic separation. Other air separation methods are considered in the literature, like adsorption, low-temperature and high-temperature membranes, or hybrid systems [5–10]. According to the recent literature, zero-emission CCPPs with oxy-combustion achieve 7–9 pp. lower efficiency than power plants without carbon capture [11–13].

High-temperature ion transport membranes (ITM) have been extensively developed over recent years. These membranes are made of ceramic materials which can conduct oxygen ions at a sufficiently high temperature (>700°C). Oxygen partial pressure difference across the membrane is the driving force for oxygen ions transport. Basically, the perovskite or fluorite membrane structures are known. In the membrane structure there are vacancies which are oxygen ion carriers, so oxygen can permeate through the membrane by passing between the voids, while the dense structure of the ceramic membranes is impermeable to other gases. This feature of ITM membranes makes it possible to produce technically pure oxygen, with an assumption of no leaks within the membrane unit [14, 15].

In CCPP a solution is considered based on replacing the combustion chamber in gas turbine with a membrane reactor, having three functions: (I) oxygen separation from compressed air by the ITM membrane; (II) heating oxygen-depleted air; (III) near-to-stoichiometric combustion of fuel. The flue gas in the membrane reactor inner cycle consists mainly of CO₂ and H₂O. The major part of the flue gas is circulated, while the rest leaves the reactor cycle, its thermal energy is utilized, then it is cooled and dried, CO₂ is

*Corresponding author

Email addresses: janusz.kotowicz@polsl.pl (Janusz Kotowicz), marcin.job@polsl.pl (Marcin Job)

compressed and transported to a place of storage. In the literature two concepts of power plants with a membrane reactor are analyzed, differentiated by the way in which energy from the flue gas leaving the membrane reactor is utilized. In the first concept the flue gas is utilized in the additional heat recovery steam generator, leading to an increase in steam turbine power [16]. In the second concept elevated pressure in the reactor cycle is applied. The flue gas is expanded in the flue gas turbine, generating additional electric power [17]. Combined cycle plants based on the membrane reactor are defined in the literature as advanced zero emission plant (AZEP). The electricity generation efficiency of both of the concepts described above is slightly above 50%.

2. Structure of the power plant

The analyzed zero-emission power plant consists of a gas turbine integrated with a membrane reactor, a steam turbine cycle with a heat recovery steam generator (HRSG), and a carbon dioxide conditioning unit. The models of all components were made using GateCycleTM software [18]. A schematic diagram of the power plant is presented in Fig. 1.

The gas turbine (GT) includes a compressor (C), a membrane reactor replacing the combustor, and a turbine (T). The compressed air is directed to the membrane reactor, where it is heated and part of the oxygen from the air permeates through the ITM membrane to the flue gas cycle. The hot, oxygen-depleted air leaving the membrane reactor is expanded in the turbine and directed to the HRSG. The expander blade air cooling model is based on the heat balance equation in the turbine blade system [19]. The cooling air is taken from the compressor outlet.

In the flue gas cycle realized in the membrane reactor, the flue gas leaving the combustor is mostly directed to the heat exchangers and ITM membrane. The flue gas, after cooling by heat exchange with air and enriched with oxygen, is sent back to the combustor as oxidant. It is assumed that in the unit the elevated flue gas pressure is at a level close to air pressure. The flue gas pressure is maintained by the fan located before the combustor. As a result of circulation, the flue gas at the combustor outlet is composed almost entirely of products of natural gas combustion, i.e. CO₂, H₂O, and excess oxygen. The uncirculated flue gas stream is chilled in a regenerative heat exchanger RHX, which does not include a membrane part, heating additional steam or air. Pre-cooled, but still hot flue gas is expanded in the flue gas turbine to a pressure close to atmospheric. The expanded flue gas is directed to the CO₂ conditioning unit, but there is a possibility of additional utilization of its low-grade heat within the power plant, depending on its temperature.

The most relevant assumptions for the gas turbine and the membrane reactor are listed in Table 1. Detailed assumptions and description regarding the ITM membrane and membrane reactor modeling are presented in Chapters 3 and 4, respectively. The turbine inlet temperature (t_{3a}) is a result of the membrane reactor calculations, and is presented in Chapter 5. The parameters of compressor inlet air

Table 1: Assumptions for gas turbine and membrane reactor

Parameter	Value
Gas turbine gross electric power, N_{elGT} , MW	200
Compressor pressure ratio, β	20
Compressor isentropic efficiency, η_{iC}	0.88
Turbines isentropic efficiency, η_{iT}, η_{iFT}	0.90
Circulation fan isentropic efficiency, η_{iF}	0.80
Mechanical efficiency of turbine and compressors, $\eta_{mT}, \eta_{mFT}, \eta_{mC}$	0.995
Electric generator efficiency, η_G	0.985
Gas turbine and steam turbine own needs, δ_{el}	0.02
Compressor inlet pressure loss rate, ζ_F	0.01
Turbine outlet pressure, p_{4a} , kPa	105.5
Combustor outlet temperature, t_{1g} , °C	1,300
Combustor outlet pressure, p_{1g} , kPa	2,000
Oxygen content in combustor outlet flue gas, (O ₂) _{1g}	0.02
Combustor heat loss rate, δ_{CMB}	0.01
Combustor pressure loss rate, ζ_{CMB}	0.04

are 15°C, 101.325 kPa and relative humidity of 60%. Combustor is fed by natural gas with 100% CH₄ content, lower heating value (LHV) equal to 50.049 MJ/kg and parameters 15°C, 3500 kPa.

The steam turbine (ST) in the model is powered through triple-pressure HRSG with reheating by oxygen-depleted air leaving the gas turbine. The maximum temperature of live steam and reheated steam depends on the HRSG inlet air temperature, with the assumption of minimum temperature difference $\Delta T \geq 20$ K. Live steam, reheated steam and low-pressure level steam pressures at the inlet of corresponding steam turbine parts are 18.0 MPa, 4.0 MPa, and 0.3 MPa, respectively. The steam turbine isentropic efficiency is assumed to be 90%.

The captured carbon dioxide before transportation to the place of storage has to be prepared in accordance with the guidelines for its composition and parameters. Minimum purity of CO₂ shall be at 90%. The flue gas brought to the carbon conditioning unit is composed primarily of CO₂, H₂O and a small amount of O₂, therefore, CO₂ capture is limited to cooling flue gas to the temperature of 30°C in the condensing heat exchanger, where the phase separation of condensed water with gaseous carbon dioxide is conducted. This process ensures the purity of CO₂ above the required 90%. This gas is stored in the form of a supercritical fluid, so compression is necessary. This step is performed in an 8-section compressor with intercooling to the temperature of 30°C. Each section has an identical pressure ratio and the CO₂ is compressed to the pressure of 13 MPa. The last section is a liquid CO₂ pump. The isentropic efficiency of the compressor is 80%. The compressed CO₂ is prepared for transport.

3. Model of the oxygen ion transport membrane (ITM)

The issue of modeling the ITM membrane includes both the processes of heat and mass transport at the membrane surface with the presence of pressure losses. It is necessary to determine the membrane surface and flux of heat transferred through the membrane. The model is based on mass

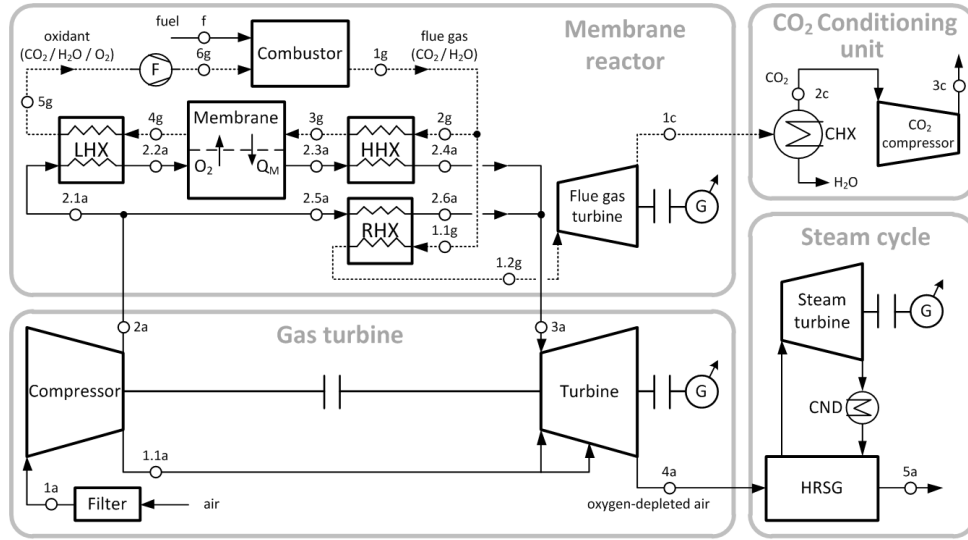


Figure 1: Scheme of the combined cycle power plant with membrane reactor AZEP (CHX—condensing heat exchanger, COND—condensator, F—circulation fan, G—generator, HRSG—heat recovery steam generator, LHX, HHX, RHX—heat exchangers)

and energy balance equations, assuming no heat losses in the membrane. Mass and energy balances on air side and flue gas side of the membrane are described by equations (1)–(4).

$$\dot{m}_{2.2a} - \dot{m}_{O_2} = \dot{m}_{2.3a} \quad (1)$$

$$\dot{m}_{2.2a} \cdot h_{2.2a} - \dot{m}_{O_2} \cdot h_{O_2} + \dot{Q}_M = \dot{m}_{2.3a} \cdot h_{2.3a} \quad (2)$$

$$\dot{m}_{3g} + \dot{m}_{O_2} = \dot{m}_{4g} \quad (3)$$

$$\dot{m}_{3g} \cdot h_{3g} + \dot{m}_{O_2} \cdot h_{O_2} - \dot{Q}_M = \dot{m}_{4g} \cdot h_{4g} \quad (4)$$

where: \dot{m}_i —mass flow of factor in point i , \dot{m}_{O_2} —mass flow of oxygen permeated through the membrane, h_i —specific enthalpy of factor in point i , \dot{Q}_M —heat flow transferred through the membrane.

The total oxygen flux through the membrane depends on two factors: an oxygen bulk diffusion, where the driving force is the gradient in the oxygen chemical potential, and oxygen surface exchange related to the oxygen partial pressure difference. For thicker membranes the oxygen flux is limited by bulk diffusion, but under characteristic membrane thickness d_c transition is controlled by surface exchange [20]. This feature indicates that above membrane characteristic thickness the Nernst-Einstein relationship (5) is valid and the oxygen flux \dot{m}_{O_2} is inversely proportional to the membrane thickness:

$$\dot{m}_{O_2} = A_M \cdot M_{O_2} \cdot \int_0^{A_M} \left\{ \frac{\sigma_i \cdot R T_M}{4d(nF)^2} \cdot \ln \left(\frac{(p_{O_2})_A}{(p_{O_2})_G} \right) \right\} dA_M \quad (5)$$

where: A_M —membrane surface, M_{O_2} —oxygen molecular weight, σ_i —oxygen ion conductivity, R —universal gas

constant ($R = 8.3145 \text{ J/mol}\cdot\text{K}$), T_M —membrane temperature, d —membrane thickness, n —charge of the charge carrier (for oxygen ions $n = 2$), F —Faraday's constant ($F = 9648.5 \text{ C/mol}$), $(p_{O_2})_A$ —oxygen partial pressure on the feed (air) side, $(p_{O_2})_G$ —oxygen partial pressure on the permeate (sweep gas) side.

From relationship (5) constant coefficient C_1 is separated, defined by the equation:

$$C_1 = \frac{R}{4d(nF)^2} \quad (6)$$

Oxygen ion conductivity σ_i is a characteristic parameter of the membrane material. The value of ion conductivity is subject to the Arrhenius temperature relation:

$$\sigma_i \cdot T_M = C_2 \cdot e^{\left(\frac{-E_a}{R T_M} \right)} \quad (7)$$

where: E_a —activation energy for ion conductivity, C_2 —constant coefficient.

The value of C_2 coefficient is determined by matching eq. (7) to the values of σ_i experimentally determined for BSCFO membrane in [15]. The values of ion conductivity are in the range $\sigma_i = 0.5 - 1.4 \text{ S/cm}$ in temperatures of 700–900°C.

On the membrane surface three phenomena take place at the same time: mass transfer, heat exchange and pressure loss. In those conditions, according to eq. (5), the oxygen flux, the membrane temperature T_M , ion conductivity σ_i , and oxygen partial pressure ratio are mutually dependent. Therefore, to determine the membrane surface A_M and other characteristic parameters, a simplified one-dimensional (1D) model is applied, in which the membrane is divided into n ($n = 100$) serially connected sections, according to the scheme shown in Fig. 2.

The main parameter defining the quantity of oxygen conducted through the membrane is the oxygen recovery ratio

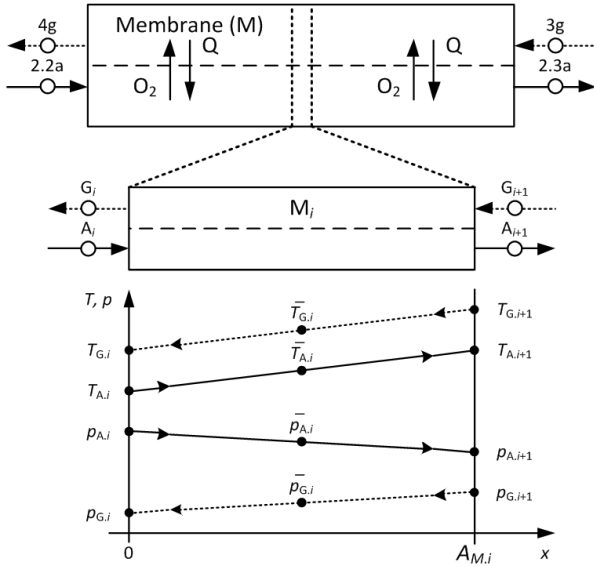


Figure 2: Schematic of the ITM membrane model

R_a :

$$R_a = \frac{\dot{m}_{O_2}}{(\dot{m}_{O_2})_{2.2a}} \quad (8)$$

where: $(\dot{m}_{O_2})_{2.2a}$ —mass flow of the oxygen in the air at the membrane inlet. Oxygen recovery ratio R_a can be also expressed on a molar basis.

Assumed in the model, equal oxygen flow is conducted through each membrane section:

$$(\dot{m}_{O_2})_i = \frac{1}{n} \cdot \dot{m}_{O_2} \quad (9)$$

where: $(\dot{m}_{O_2})_i$ —oxygen mass flow conducted through i membrane section, n —number of membrane sections ($n = 100$).

A number of simplifications are introduced in the model in order to identify parameters depending on temperature and pressure (Fig. 2):

- fixed, arithmetic mean temperatures of air $\bar{T}_{A,i}$ and flue gas $\bar{T}_{G,i}$ in i membrane section,
- fixed i membrane section temperature $T_{M,i}$, equal to the arithmetic average of temperatures $\bar{T}_{A,i}$ and $\bar{T}_{G,i}$.
- fixed, arithmetic mean total pressure of air $\bar{p}_{A,i}$ and flue gas $\bar{p}_{G,i}$ in i membrane section,
- linear change of the oxygen molar fraction in air and flue gas with the membrane surface.

Taking into account eq. (6), eq. (7) and the simplification presented above, eq. (5) for each membrane section takes the form:

$$(\dot{m}_{O_2})_i = A_{M,i} \cdot M_{O_2} \cdot C_1 \cdot C_2 \cdot e^{\left(\frac{-E_a}{RT_{M,i}}\right)} \cdot \int_0^{A_{M,i}} \ln \left(\frac{(p_{O_2})_A}{(p_{O_2})_G} \right) dA_{M,i} \quad (10)$$

Geometry of the membrane is not examined. With the assumption of constant shape of membrane module channels, the membrane surface can be treated as dependent on linear parameter x . The derivative of the membrane surface is determined:

$$\frac{dA_M}{A_M} = \frac{dx}{x} \quad (11)$$

The oxygen partial pressure ratio from eq. (10) can be written as:

$$\frac{(p_{O_2})_A}{(p_{O_2})_G} = \beta_{M,i} \cdot \frac{(x_{O_2})_A}{(x_{O_2})_G} \quad (12)$$

where: $(x_{O_2})_A$ —oxygen molar fraction in air, $(x_{O_2})_G$ —oxygen molar fraction in flue gas. The oxygen molar fractions in air and flue gas, respectively, can be expressed as linear functions:

$$(x_{O_2})_A = y_1 = a_1 \cdot x + b_1 \quad (13)$$

$$(x_{O_2})_G = y_2 = a_2 \cdot x + b_2 \quad (14)$$

where: a_1, a_2, b_1, b_2 —coefficients of linear function. Introduction of eqs. (11)–(14) into eq. (10) leads to:

$$(\dot{m}_{O_2})_i = A_{M,i} \cdot M_{O_2} \cdot C_1 \cdot C_2 \cdot e^{\left(\frac{-E_a}{RT_{M,i}}\right)} \int_0^{A_{M,i}} \ln \left[\beta_{M,i} \cdot \frac{(a_1 \cdot x + b_1)}{(a_2 \cdot x + b_2)} \right] dx \quad (15)$$

Values of coefficients a_1, b_1, a_2, b_2 are determined separately for each membrane section, according to the formulas:

$$a_{1,i} = \frac{(x_{O_2})_{A,i+1} - (x_{O_2})_{A,i}}{A_{M,i}} \quad (16)$$

$$b_{1,i} = (x_{O_2})_{A,i} \quad (17)$$

$$a_{2,i} = \frac{(x_{O_2})_{G,i+1} - (x_{O_2})_{G,i}}{A_{M,i}} \quad (18)$$

$$b_{2,i} = (x_{O_2})_{G,i} \quad (19)$$

By solving the integral from eq. (15), introduction of eqs. (16)–(19), and making transformations, the relationship describing the surface of the i membrane section takes the form:

$$A_{M,i} = \frac{(\dot{m}_{O_2})_i \cdot \left[M_{O_2} \cdot C_1 \cdot C_2 \cdot e^{\left(\frac{-E_a}{RT_{M,i}}\right)} \right]^{-1}}{\ln \beta_{M,i} + \ln \left(\frac{(x_{O_2})_{A,i+1}}{(x_{O_2})_{G,i+1}} \right) + D_{1,i} + D_{2,i}} \quad (20)$$

$$D_{1,i} = \frac{(x_{O_2})_{A,i}}{(x_{O_2})_{A,i+1} - (x_{O_2})_{A,i}} \cdot \ln \left(\frac{(x_{O_2})_{A,i+1}}{(x_{O_2})_{A,i}} \right) \quad (21)$$

$$D_{2,i} = \frac{(x_{O_2})_{G,i}}{(x_{O_2})_{G,i+1} - (x_{O_2})_{G,i}} \cdot \ln \left(\frac{(x_{O_2})_{G,i}}{(x_{O_2})_{G,i+1}} \right) \quad (22)$$

Table 2: Characteristic parameters of ITM membrane material

Parameter	Value
Minimum operation temperature of membrane, $(t_M)_{min}$, °C	700
Maximum operation temperature of membrane, $(t_M)_{max}$, °C	900
Heat transfer coefficient of membrane, k_M , W/m ² K	90
Minimum membrane thickness including porous support, mm	0.5
Characteristic membrane thickness, d_c , mm	0.1
Activation energy for ion conductivity, E_a , kJ/mol	56
Constant coefficient for ion conductivity, C_2	517,000

Knowing the i membrane section surface $A_{M,i}$, in the following step the heat flow exchanged through this surface $\dot{Q}_{M,i}$ can be determined using the equation:

$$\dot{Q}_{M,i} = k_M \cdot A_{M,i} \cdot \Delta T_{M,i} \quad (23)$$

where: k_M —heat transfer coefficient of the membrane, $\Delta T_{M,i}$ —logarithmic mean temperature difference in the membrane.

The use of ITM membranes with thickness lower than characteristic thickness d_c does not result in significant growth of oxygen flux. The majority of known perovskite membranes have characteristic thickness of 50 to 100 μm . Such thin membranes are already produced, but they have to be strengthened by a porous support to provide mechanical stability, especially taking into account the high pressure differences on both sides of the membrane. The porous support is made of the same or similar material as the membrane, but they are sintered at lower temperatures to provide suitable porosity. Therefore, the porous support does not accept high operation temperatures, which make them sinter and reduce their porosity, resulting in degradation of membrane performance. Perovskites are the most widely studied and developed group of materials for ITM membranes. The results presented in [21] indicate that perovskite porous support should withstand an absolute pressure difference of 3.0 MPa, but application of temperatures equal to or higher than 1000°C reduce its porosity due to significant sintering at such temperatures.

BSCFO ($\text{Ba}_{0.5}\text{Sr}_{0.5}\text{Co}_{0.8}\text{Fe}_{0.2}\text{O}_{2-d}$) material, which receives special mention in the literature, is characterized by high oxygen conductivity compared to other materials [14, 15, 21]. Characteristic parameters of BSCFO, based on data from [15, 20] and presented in Table 2, are also applied in the presented membrane model. Calculations in the membrane model are performed iteratively due to the interdependence of the membrane surface, the temperatures and pressure losses of gases. A block diagram of calculation algorithm for the ITM membrane model is presented in Fig. 3.

4. Model of the membrane reactor

In the presented model an integrated structure of the membrane module (LHX-M-HHX) is assumed. In the module the membrane is located between two heat exchangers: low-temperature LHX and high-temperature HHX. One of the

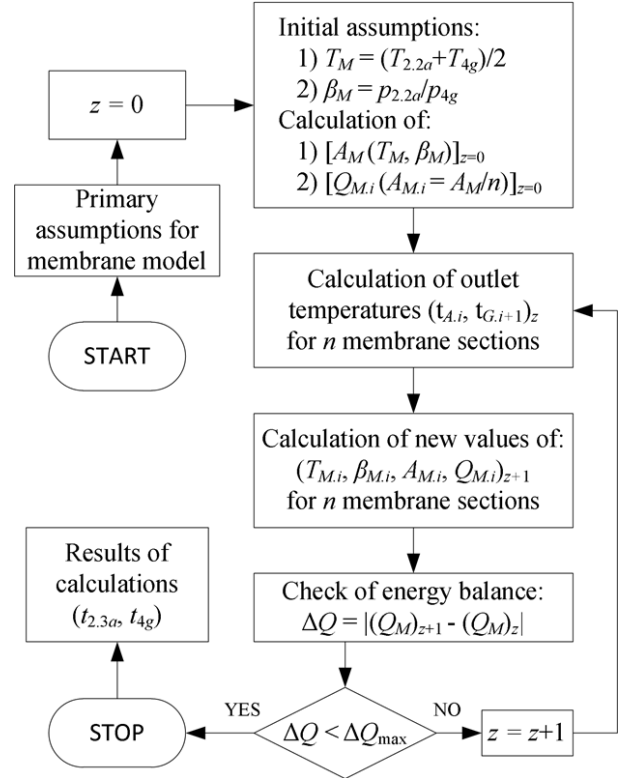


Figure 3: Block diagram of calculation algorithm for ITM membrane model

principal limitations for heat exchangers is the maximum applicable temperature of flue gas, which is currently at the level of 1300°C for ceramic heat exchangers [16].

Flue gas temperatures at the inlet (t_{2g}) and outlet (t_{3g}) of HHX are assumed in the model. Air temperature at the HHX inlet ($t_{2.3a}$) is provided by the membrane model, while HHX outlet air temperature ($t_{2.4a}$) is calculated on the basis of the energy balance for HHX.

Air temperatures at the LHX inlet ($t_{2.1a}$) and outlet ($t_{2.2a}$) are known. The flue gas temperature at the LHX inlet (t_{4g}) is a result of the membrane model calculations, while LHX outlet flue gas temperature (t_{5g}) is calculated on the basis of the energy balance for LHX.

The flue gas at regenerative heat exchanger RHX inlet has a temperature equal to the combustor outlet temperature ($t_{1c} = t_{1g}$). Air temperatures at the RHX inlet and outlet are equal to LHX inlet air temperature ($t_{2.5a} = t_{2.1a}$) and HHX outlet air temperature ($t_{2.6a} = t_{2.4a}$), respectively. Flue gas temperature at the RHX outlet is assumed in the model, while air flow $\dot{m}_{2.5a}$ is calculated on the basis of the RHX energy balance.

To avoid determining detailed membrane geometry, a simplified pressure losses distribution is implied in the presented model. Constant pressure loss ratios in the membrane reactor on air side ξ_A and flue gas side ξ_G are introduced. Pressure losses distribution in all components of membrane modules are important for proper determination of oxygen partial pressures on both sides of the ITM membrane. Analyses presented in [20] concluded that, for the membrane struc-

Table 3: Assumptions for membrane reactor

Parameter	Value
Combustor outlet temperature, t_{1g} , °C	1,300
RHX outlet flue gas temperature, t_{2c} , °C	600
Combustor outlet pressure, p_{2g} , MPa	2.0
Circulation fan isentropic efficiency, η_w	0.80
Thermal efficiency of heat exchangers, η_{LHX} , η_{HHX} , η_{RHX}	0.995
Air pressure loss rate in membrane modules, ξ_A	0.125
Flue gas pressure loss rate in membrane modules, ξ_G	0.125
Pressure loss distribution, %:	
- inlet flow converter (IN):	60
- membrane module (MOD):	20
- outlet flow collector (OUT):	20
Heat transfer coefficient of LHX, k_{LHX} , W/m ² K	70
Heat transfer coefficient of HHX, k_{HHX} , W/m ² K	100
Heat transfer coefficient of RHX, k_{RHX} , W/m ² K	90
Minimum temperature difference in heat exchangers, K	20

ture shown in [16], the highest pressure losses are bound with separation and distribution of gas flows. Thus, the inlet flow converter is responsible for about 60% and outlet flow collector for about 20% of total pressure losses, while only 20% of total pressure losses is generated in channels of membrane modules. The total relative pressure losses in membrane modules are at the level of 12–14%, according to [10, 22]. Total pressure losses are divided in the model according to the equation:

$$\Delta p_i = \Delta p_{i.IN} + \Delta p_{i.MOD} + \Delta p_{i.OUT} \quad (24)$$

where: Δp_i —total absolute pressure loss; ($i = A, G$), IN—inlet flow converter of membrane module, MOD—membrane module (LHX-M-HHX/ RHX), OUT—outlet flow collector of membrane module.

Pressure losses for each membrane module component are divided proportionally to its surface:

$$\Delta p_{i,j} = \Delta p_{i.MOD} \cdot \frac{A_j}{\sum A_j} \quad (25)$$

where: $j = LHX, M, HHX$.

Pressure losses in RHX are the same as in the membrane module ($\Delta p_{j.RHX} = \Delta p_{j.MOD}$), since it has the same structure. Surface areas of HHX, LHX and RHX are calculated using heat transfer coefficients k , based on eq. (23). Values of heat transfer coefficients are assumed individually for each heat exchanger on the basis of data presented in [20].

Oxygen recovery rate R_a (eq. (8)) and flue gas flow rate γ_G are primary parameters responsible for regulation of the flue gas cycle in the membrane reactor. The flue gas flow rate γ_G is a ratio of the membrane inlet flue gas mass flow to the membrane inlet air mass flow, described by the equation:

$$\gamma_G = \frac{\dot{m}_{3g}}{\dot{m}_{2.2a}} \quad (26)$$

The value of the oxygen recovery rate in ITM membrane R_a is controlled for the assumed value of γ_G to achieve constant oxygen content in the combustor outlet flue gas of 2%. The most important assumptions for the membrane reactor are set down in Table 3. Calculations of the membrane reactor model for the assumed γ_G value are conducted according to the algorithm presented in Fig. 4.

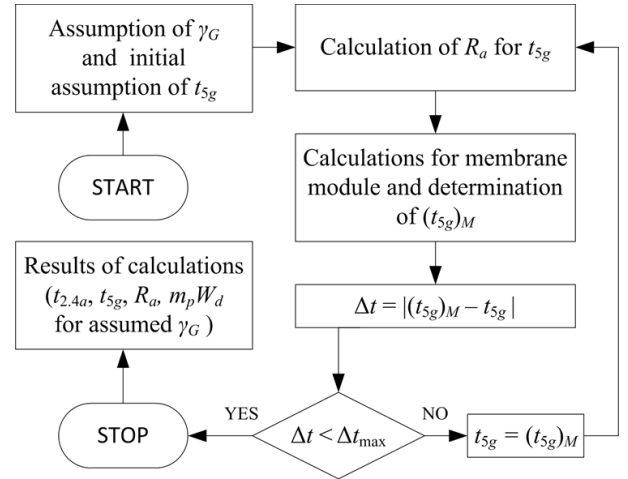
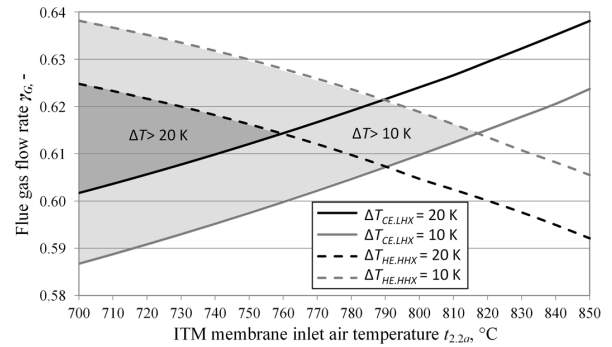


Figure 4: Block diagram of calculation algorithm for membrane reactor


 Figure 5: Range of applicable γ_G values due to minimum temperature differences in heat exchangers $\Delta T_{CE.LHX}$ and $\Delta T_{HE.HHX}$ as a function of membrane inlet air temperature $t_{2.2a}$

5. Thermodynamic analysis of the power plant

In the first place an analysis of the membrane reactor was made in order to select the operating parameters for integration with the gas turbine. The impact of flue gas flow rate γ_G and membrane inlet air temperature on the membrane working conditions were analyzed. The range of acceptable γ_G values is limited by an assumption of minimum temperature difference at the ends of the membrane module. Presented in Fig. 5 are the resulting temperature differences at the cold end of LHX ($\Delta T_{CE.LHX}$) and at the hot end of HHX ($\Delta T_{HE.HHX}$) as a function of membrane inlet air temperature ($t_{2.2a}$), with the indicated range of acceptable γ_G values resulting from the temperature limitations (dark grey area on Fig. 5).

The surface areas of the ITM membrane and heat exchangers are significant for both external dimensions of the membrane reactor and investment costs. The surface areas of the heat exchangers are the lowest in a range of the highest temperature differences. The increase in membrane inlet air temperature $t_{2.2a}$ results in a slight reduction of ITM membrane surface area, but a simultaneous significant increase in the heat exchangers' areas. Membrane module designs achieve a high density of active area per volume of

Table 4: Results of membrane reactor analysis

Parameter	Value
$t_{5g}, ^\circ\text{C}$	469.9
$t_{4g}, ^\circ\text{C}$	733.7
$t_{3g}, ^\circ\text{C}$	900.0
$t_{2g}, ^\circ\text{C}$	1300.0
$t_{2c}, ^\circ\text{C}$	600.0
$t_{1c}, ^\circ\text{C}$	1300.0
$t_{2.1a}, ^\circ\text{C}$	442.0
$t_{2.2a}, ^\circ\text{C}$	700.0
$t_{2.3a}, ^\circ\text{C}$	863.6
$t_{2.4a}, ^\circ\text{C}$	1271.9
$t_{2.5a}, ^\circ\text{C}$	442.0
$t_{2.6a}, ^\circ\text{C}$	1271.9
A_{LHX}, m^2	67 336
A_M, m^2	29 520
A_{HHX}, m^2	70 532
A_{RHX}, m^2	9 978

400 to even over 1000 m^2/m^3 . Based on the obtained results, values of $\gamma_G = 0.614$ and $t_{2.2a} = 700^\circ\text{C}$ are assumed for the power plant analysis. For selected parameters the oxygen recovery rate is $R_a = 0.3787$, while the obtained temperatures and surface areas of ITM membrane and heat exchangers are presented in Table 4.

In order to evaluate the analyzed power plant gross electricity generation efficiency $\eta_{el.gr}$ is calculated according to equation:

$$\eta_{el.gr} = \frac{N_{el.gr}}{\dot{m}_f LHV} = \frac{N_{elGT} + N_{elST} + N_{elFT}}{\dot{m}_f LHV} \quad (27)$$

where: $N_{el.gr}$ —gross electric power of power plant, N_{elGT} —gas turbine electric power, N_{elST} —steam turbine electric power, N_{elFT} —flue gas turbine electric power, $\dot{m}_f LHV$ —fuel chemical energy flux (lower heating value basis).

Gas turbine electric efficiency η_{elGT} and steam turbine electric efficiency η_{elST} are described by formulas:

$$\eta_{elGT} = \frac{N_{elGT} + N_{elFT}}{\dot{m}_f LHV} \quad (28)$$

$$\eta_{elST} = \frac{N_{elST}}{\dot{Q}_{4a}} \quad (29)$$

where: \dot{Q}_{4a} —HRSG inlet air heat flow.

The net efficiency of electricity generation for power plant is calculated by analogy to eq. (27), taking into account own needs of individual installations within the power plant, i.e., gas turbine and steam turbine ΔN_{el} , carbon dioxide conditioning unit ΔN_{CC} and circulation fan in the membrane reactor ΔN_F :

$$\eta_{el} = \frac{N_{elGT} + N_{elST} + N_{elFT}}{\dot{m}_f LHV} - \frac{\Delta N_{el} + \Delta N_{CC} + \Delta N_F}{\dot{m}_f LHV} \quad (30)$$

Primary thermodynamic parameters, indicators and own needs of all installations in the AZEP plant are determined in the thermodynamic analysis. The temperature of HRSG inlet air is 536°C , therefore the assumed live steam and reheated steam temperatures are 515°C . A classic combined

 Table 5: Characteristic parameters of power plants (AZEP - combined cycle power plant with membrane reactor, CCGP - reference combined cycle power plant without CO_2 capture)

Parameter	AZEP	CCPP
Turbine internal power N_{IT} , MW	500.9	421.6
Compressor internal power N_{iC} , MW	293.9	215.3
Gas turbine electric power N_{elGT} , MW	200.0	200.0
Flue gas turbine electric power N_{elFTS} , MW	30.7	–
Fuel chemical energy flux $\dot{m}_f LHV$, MW	584.8	496.6
Electric efficiency of gas turbine η_{elGT} , -	0.3946	0.4027
HRSG inlet heat flow \dot{Q}_{4a} , MW	337.1	285.1
Steam turbine electric power N_{elST} , MW	106.7	91.1
Electric efficiency of steam turbine η_{elST} , -	0.3165	0.3195
Gross electric power $N_{el.gr}$, MW	337.4	291.1
Gross electricity generation efficiency $\eta_{el.gr}$, -	0.5770	0.5862
Gas turbine and steam turbine own needs ΔN_{el} , MW	6.7	5.8
CO_2 conditioning unit own needs ΔN_{CC} , MW	10.7	–
Circulation fan own needs ΔN_W , MW	19.4	–
Net electric power N_{el} , MW	300.6	285.3
Net electricity generation efficiency η_{el} , -	0.5140	0.5745
Carbon dioxide production u_{CO_2} , kg/MWh	384.0	346.5
Carbon dioxide emission e_{CO_2} , kg/MWh	≈ 0.0	346.5

cycle power plant without CO_2 capture (CCPP) is also analyzed as a reference unit for comparison. In CCGP identical parameters of gas turbine ($t_{3a} = 1271.9^\circ\text{C}$, $\beta = 20$) are assumed. The temperature of HRSG inlet flue gas in this case is 540°C , which resulted in slightly higher steam temperatures (520°C). The most relevant results of thermodynamic analyses for both power plants are presented in Tab. 5.

In the gas turbine integrated with a membrane reactor the mass flow of oxygen-depleted air powering the expander is lower than the compressed air mass flow, by the amount of oxygen conducted through the membrane, and consequently gas turbine efficiency is about 6 pp. lower than in the classic design. However, including the additional electric power generated by turbine fed by flue gas from the membrane reactor, the efficiency gap is reduced to less than 1 pp. The steam turbine efficiency is similar in both power plants. The 6% reduction in net electric efficiency experienced by AZEP in relation to reference plant CCGP is primarily caused by the significant own needs of the circulation fan and CO_2 conditioning unit.

6. Conclusions

A model of a membrane reactor integrated with a combined cycle gas turbine unit was made. The presented results of a thermodynamic analysis identified the basic features of this carbon dioxide capture technology.

The lower electric efficiency of the gas turbine with a membrane reactor, vis-à-vis the classic gas turbine, is partly compensated by an additional turbine fed by flue gas leaving the membrane reactor. The AZEP achieved gross electricity generation efficiency of 57.7%. The significantly lower net efficiency (51.4%) is primarily due to the high own needs of the circulation fan in the membrane reactor (19.4 MW) and of the CO_2 conditioning unit (10.7 MW). There is a 6 pp. resulting reduction in net electric efficiency related to the reference power plant.

State-of-art combined cycle power plants, through the use of higher combustor outlet temperatures, at the level of 1600°C, achieve net electric efficiency above 60%. Compared to these values, the net electric efficiency of AZEP would be lower by 8–9 pp. These are values recently comparable with combined cycle power plants with CO₂ capture in post-combustion technology.

Future potential for development of power plants with membrane reactors is dependent on the maximum applicable temperature, which is currently restricted by heat exchangers to the level of about 1300°C. Development of ITM membrane materials is also important, in terms of improving their chemical characteristics (ion conductivity) and mechanical stability (the ability to use higher temperatures). Improving these parameters would lead to a significant reduction in the surface of the ITM membrane itself (in the discussed power plant approx. 30000 m²), but also heat exchangers (total approx. 150000 m²). High pressure losses in the membrane reactor of over 12% are also disadvantageous. The development of optimized designs for elements within the reactor to reduce the pressure losses will improve the efficiency of AZEP.

Acknowledgments

The article was written within statutory research funds of Silesian University of Technology

References

- [1] R. K. Pachauri, M. R. Allen, V. Barros, J. Broome, W. Cramer, R. Christ, J. Church, L. Clarke, Q. Dahe, P. Dasgupta, et al., *Climate change 2014: synthesis Report. Contribution of working groups I, II and III to the fifth assessment report of the intergovernmental panel on climate change*, IPCC, 2014.
- [2] *Energy and climate change, World energy outlook special report*, International Energy Agency (2015).
- [3] T. Chmielniak, *Energy technologies*, WNT, Warsaw, 2008.
- [4] K. Badyda, *Perspektywy rozwoju technologii turbin gazowych oraz bloków gazowo-parowych [state and prospects of gas turbine and combined cycle technology development]*, *Rynek Energii* 4 (113) (2014) 74–82.
- [5] J.-P. Tranier, R. Dubettier, A. Darde, N. Perrin, *Air separation, flue gas compression and purification units for oxy-coal combustion systems*, *Energy Procedia* 4 (2011) 966–971.
- [6] L. Zheng (Ed.), *Oxy-fuel combustion for power generation and carbon dioxide (CO₂) capture*, Woodhead Publishing Limited, 2011.
- [7] A. R. Smith, J. Klosek, *A review of air separation technologies and their integration with energy conversion processes*, *Fuel processing technology* 70 (2) (2001) 115–134.
- [8] J. Kotowicz, S. Michalski, *Efficiency analysis of a hard-coal-fired supercritical power plant with a four-end high-temperature membrane for air separation*, *Energy* 64 (2014) 109–119.
- [9] T. Burdyny, H. Struchtrup, *Hybrid membrane/cryogenic separation of oxygen from air for use in the oxy-fuel process*, *Energy* 35 (5) (2010) 1884–1897.
- [10] E. Yantovsky, J. Górski, M. Shokotov, *Zero emissions power cycles*, CRC Press, 2009.
- [11] C. Liu, G. Chen, N. Sipöcz, M. Assadi, X.-S. Bai, *Characteristics of oxy-fuel combustion in gas turbines*, *Applied Energy* 89 (1) (2012) 387–394.
- [12] N. Zhang, N. Lior, *Two novel oxy-fuel power cycles integrated with natural gas reforming and CO₂ capture*, *Energy* 33 (2) (2008) 340–351.
- [13] J. Kotowicz, M. Job, M. Brzęczek, *Porównanie termodynamiczne elektryczności gazowo-parowych bez iz wychwytem CO₂*, *Rynek Energii* 112 (2014) 82–87.
- [14] K. Foy, J. McGovern, *Comparison of ion transport membranes*, in: *Proc. 4th Annual Conference on Carbon Capture and Sequestration*, 2005, pp. 2–5.
- [15] H. Lu, Y. Cong, W. Yang, *Oxygen permeability and stability of Ba_{0.5}Sr_{0.5}Co_{0.8}Fe_{0.2}O_{3-δ} as an oxygen-permeable membrane at high pressures*, *Solid State Ionics* 177 (5) (2006) 595–600.
- [16] S. G. Sundkvist, S. Julsrud, B. Vigeland, T. Naas, M. Budd, H. Leistner, D. Winkler, *Development and testing of AZEP reactor components*, *International Journal of Greenhouse Gas Control* 1 (2) (2007) 180–187.
- [17] H. M. Kvamsdal, K. Jordal, O. Bolland, *A quantitative comparison of gas turbine cycles with CO₂ capture*, *Energy* 32 (1) (2007) 10–24.
- [18] GE Enter Software, LLC, *GateCycle Version 5.40. Manual*.
- [19] J. Kotowicz, M. Job, M. Brzęczek, *The characteristics of ultramodern combined cycle power plants*, *Energy* 92 (2015) 197–211.
- [20] F. Selimovic, *Computational analysis and modeling techniques for monolithic membrane reactors related to CO₂ free power processes*, Ph.D. thesis, University of Lund, Sweden (2007).
- [21] M. van der Haar, *Mixed-conducting perovskite membranes for oxygen separation. Towards the development of a supported thin-film membrane*, Ph.D. thesis, University of Twente, Enschede, Netherlands (2001).
- [22] K. F. R. Warcholand, J. McGovern, *A detailed simulation of the zeitrom cycle with combined air separation and combustion*, *Proc. of ECOS* (2007) 25–28.